

Effect of Ga doping on the multiferroic properties of $RMn_{1-x}Ga_xO_3$ ($R=Ho, Y$)

H. D. Zhou, J. C. Denyszyn, and J. B. Goodenough

Texas Materials Institute, ETC 9.102, The University of Texas at Austin, 1 University Station, C2201, Austin, Texas 78712, USA

(Received 1 September 2005; revised manuscript received 14 October 2005; published 1 December 2005)

Structural, thermal expansion, thermal conductivity, magnetic, and dielectric measurements on single-crystal $RMn_{1-x}Ga_xO_3$ ($R=Ho$ or Y) hexagonal compounds have revealed that the c axis decreases with increasing temperature with a larger $|dc/dT|$ above T_C than below it, which shows that the cooperative MnO_5 site rotations responsible for the ferrielectricity expend energy to induce the ferroic R^{3+} -ion displacements along the c axis. Ga doping raises the ferrielectric Curie temperature T_C and the Mn-spin reorientation temperature T_{SR} while lowering T_N of the Mn spins and the Ho magnetic ordering temperature T_2 . The data show an important coupling between the Mn^{3+} -ion and Ho^{3+} -ion spins as well as a T_{SR} that is driven by the cooperative MnO_5 site rotation and R^{3+} -ion displacements that control the c lattice parameter. The data also support an enhanced spin-lattice interaction in the geometrically frustrated Mn-spin system.

DOI: 10.1103/PhysRevB.72.224401

PACS number(s): 75.47.Lx, 77.80.-e, 66.70.+f, 65.40.De

I. INTRODUCTION

The $RMnO_3$ compounds with smaller rare-earth ions (R from Ho to Lu and Y) have attracted considerable recent attention because of the coexistence of ferrielectricity and antiferromagnetic order with a coupling between them. The high-temperature hexagonal $P6_3/mmc$ structure contains close-packed planes of Mn^{3+} ions in bipyramidal oxygen coordination separated by planes of R^{3+} ions. A cooperative rotation of the bipyramidal axis from the c axis below a temperature T_l loses the mirror planes perpendicular to the c axis and changes the symmetry to $P6_3cm$. These rotations also induce a ferrielectric displacement of the R^{3+} ions along the c axis below a Curie temperature $T_C < T_l$ without a further change in crystal symmetry.¹ The dominant spin-spin interactions between Mn^{3+} ions within the close-packed basal planes are geometrically frustrated (GF), which lowers the antiferromagnetic ordering temperature T_N of the Mn^{3+} ions to a $T_N \ll T_C$. Any magnetic moment on the R^{3+} ions becomes long-range ordered only below a $T_2 \ll T_N$. A reorientation of the Mn^{3+} -ion spins occurs at a T_{SR} ; the spin reorientation appears to be induced by a coupling between the ferrielectricity and the antiferromagnetic order since $T_2 < T_{SR} < T_N$. These five transitions are found, for example, in $HoMnO_3$, which has a $T_C=875$ K.² Below $T_N \approx 70$ K, the magnetic symmetry changes to $P\bar{6}_3cm$ with Mn spins in the basal planes perpendicular to an a axis oriented at 120° with respect to their nearest neighbors and out of phase between planes.³ A 90° rotation of the Mn spins in the basal planes to along an a axis at $T_{SR} \approx 40$ K (Ref. 4) or 33 K (Ref. 5) changes the magnetic symmetry to $P\bar{6}_3cm$.³ At $T_2 \approx 5$ K, another 90° rotation of the Mn spins in the basal planes, but in phase between planes, gives the magnetic symmetry $P6_3cm$; this spin reorientation is accompanied by a magnetic ordering of the Ho^{3+} -ion spins orientated along the c axis. $YMnO_3$ has a $T_C=915$ K (Ref. 2) or 935 K (Ref. 6) and a $T_N \approx 70$ K.

Recent work on these $RMnO_3$ compounds has been focused on the following subjects: (i) the magnetic symmetry and magnetic phases at low temperatures;^{3-5,7-12} (ii) the coupling between the ferrielectric and magnetic orderings; anomalies of the dielectric constant at the three magnetic

transitions clearly show a significant coupling;¹³⁻¹⁶ and (iii) the strong spin-lattice interaction of the GF Mn-spin system.¹⁷ Most of these studies have been performed on $HoMnO_3$ and $YMnO_3$, which means the several ordering temperatures associated with a given R^{3+} ion are fixed.

In this paper, we substitute Ga for Mn in single crystals of $RMn_{1-x}Ga_xO_3$ ($R=Ho$ or Y) in order to see how, for a given R^{3+} ion, the several transition temperatures vary with respect to one another and also how the spin-lattice interactions above T_N change with increasing x . We also monitor the temperature variation of the c axis above and below T_C to investigate how the cooperative rotations of the MnO_5 bipyramidal sites responsible for the ferrielectricity are affected by the forced ferroic displacements of the R^{3+} ions.

II. EXPERIMENTAL

Single crystals of $RMn_{1-x}Ga_xO_3$ ($R=Ho, Y$ and $x=0, 0.03, 0.1, \text{ and } 0.2$) were grown by the traveling-solvent floating-zone (TSFZ) technique. The feed and seed rods for the crystal growth were prepared by solid-state reaction. Stoichiometric mixtures of $Ho_2O_3/Y_2O_3, Mn_2O_3, \text{ and } Ga_2O_3$ were ground together and calcined in air at $950^\circ C$ for 24 h. The sample was reground and sintered at $1100^\circ C$ for another 24 h in air and cooled to room temperature. It was then reground again into a powder and pressed into a 6-mm-diameter \times 60-mm rod under 400 atm hydrostatic pressure. The rods were finally sintered at $1200^\circ C$ for 20 h in air. The crystal growth was carried out in air in an IR-heated image furnace (NEC) equipped with two halogen lamps and double ellipsoidal mirrors. The feed and seed rods were rotated in opposite directions at 25 rpm during crystal growth at a rate of 4 mm/h.

Small pieces of the single crystals were ground into fine powder for x-ray diffraction (XRD). The room-temperature measurements were recorded with an X-pert Philips diffractometer equipped with $Cu K\alpha$ radiation. Data were collected in steps of 0.02° over the range $10^\circ \leq 2\theta \leq 90^\circ$ with a count time of 5 s per step. High temperature measurements were recorded with a Scintag theta-theta diffractometer with a solid-state detector and $Cu K\alpha$ radiation. The sample was

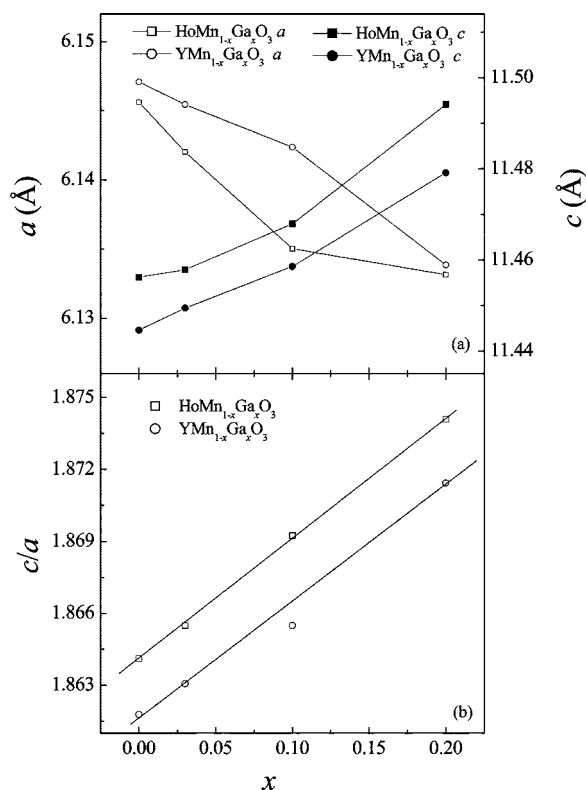


FIG. 1. Variation with x of (a) lattice parameters and (b) c/a ratio for $RMn_{1-x}Ga_xO_3$ ($R=Ho$ or Y and $0 \leq x \leq 0.2$) at room temperature.

heated on a Pt-Rh strip under flowing N_2 gas. Peak profiles were fitted with the program JADE. X-ray Laue diffraction was used to orient the crystal.

Bars cut from the single crystals for magnetic and thermal conductivity measurements had a typical size of $0.5 \times 0.5 \times 3$ mm³ with the longest dimension parallel to either the a - b plane or the c axis. The magnetic-susceptibility measurements were made with a Quantum Design dc superconducting quantum interference device (SQUID) magnetometer with an applied field of 100 Oe; the measurements were made on heating after cooling in zero field (ZFC). The thermal conductivity $\kappa(T)$ was measured in the temperature region 7–300 K with a steady-state heat-flow technique having a systematic error less than 20%.

Thermal expansion measurements were performed on a Perkin-Elmer Series 7 Thermomechanical Analyzer (TMA). The samples had a typical size of $1 \times 1 \times 3$ mm³ with the longest dimension parallel to the c axis.

The dielectric constant ϵ along the c direction was obtained from the capacitance of the sample by an impedance analyzer (HP 4192A) with frequency 500 kHz.

III. RESULTS

All samples were single-phase to XRD with the hexagonal $P6_3cm$ structure at room temperature. Both for $HoMn_{1-x}Ga_xO_3$ and $YMn_{1-x}Ga_xO_3$, the lattice parameter a decreases and c increases with increasing x as shown in Fig. 1.

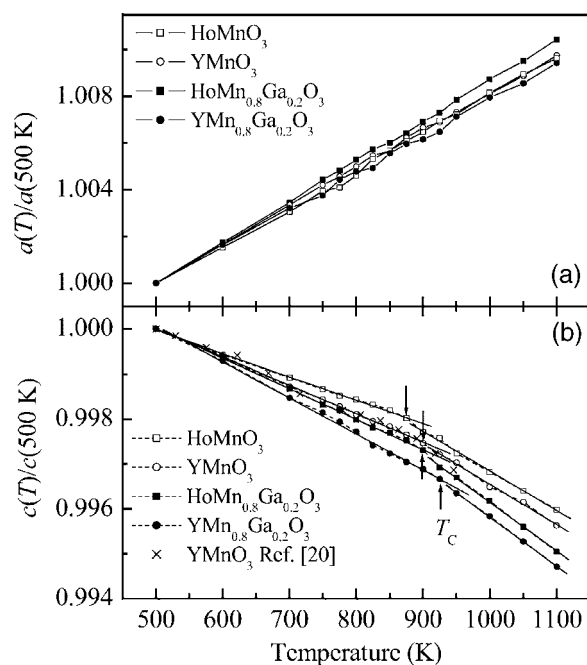


FIG. 2. Temperature dependences of lattice parameters (a) a and (b) c , both of which are normalized to the values at 500 K, for $RMn_{1-x}Ga_xO_3$ ($R=Ho$ or Y , $x=0$ and 0.2). Solid lines of (b) are linear fittings.

Figure 2 shows the high-temperature (500 K to 1100 K) dependences of the lattice constants for four samples: $HoMnO_3$, $HoMn_{0.8}Ga_{0.2}O_3$, $YMnO_3$, and $YMn_{0.8}Ga_{0.2}O_3$. The in-plane lattice constant shows a linear increase with increasing temperature. On the other hand, the c lattice constant decreases with increasing temperature, and there are slope changes around 875 K, 900 K, 900 K, and 925 K for $HoMnO_3$, $HoMn_{0.8}Ga_{0.2}O_3$, $YMnO_3$, and $YMn_{0.8}Ga_{0.2}O_3$, respectively.

Figure 3 shows the TMA thermal expansion measurements along the c direction. The results are similar to those obtained from the XRD measurements. All samples show a negative c -axis thermal expansion and have slope changes around 900 K as were also obtained from XRD. Both for $HoMn_{1-x}Ga_xO_3$ and $YMn_{1-x}Ga_xO_3$, the temperature of the slope change increases with increasing x (inset of Fig. 3). Due to the limitation of our TMA, the calculated value $L(T)/L(500\text{ K})$ is smaller than the value $c(T)/c(500\text{ K})$ obtained from XRD. In the discussion below, the thermal expansion coefficients were calculated from the XRD results.

Figure 4(a) shows the temperature dependences of $d(1/\chi_{||})/dT$ for $HoMn_{1-x}Ga_xO_3$ over the temperature range $25\text{ K} < T < 60\text{ K}$; $\chi_{||}$ is the susceptibility measured along the c axis. For all samples, the derivatives show a peak around $T_{SR} \approx 40\text{ K}$ that is due to Mn spin-reorientation. With increasing x , T_{SR} increases [inset of Fig. 4(a)]. At the same time, the dielectric constants measured along the c axis of $HoMn_{1-x}Ga_xO_3$ show sharp peaks around T_{SR} , but the peak's intensity decreases with increasing x , as shown in Fig. 4(b). A difference of less than 1 K between the temperatures of the magnetic anomaly and the dielectric peak may be due to the following experimental differences: (i) although the

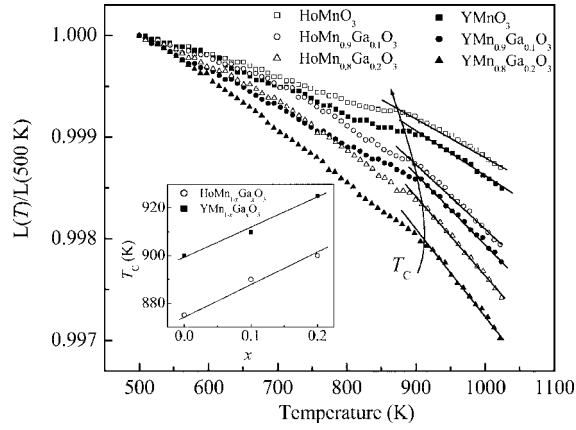


FIG. 3. Thermal expansion along the c axis for $\text{RMn}_{1-x}\text{Ga}_x\text{O}_3$ ($R=\text{Ho}$ or Y , $x=0, 0.1$, and 0.2). Solid lines are guides to the eye. Inset: Variation with x of T_C for $\text{RMn}_{1-x}\text{Ga}_x\text{O}_3$.

samples for susceptibility and dielectric constant measurements were cut from the same single crystal, the orientations were separately performed; (ii) the susceptibility was measured on a SQUID cooled by liquid He, but the dielectric constants were measured on a homemade setup cooled by a He refrigerating cryostat.

Figure 5 shows the temperature dependences of $d(1/\chi_{||})/dT$ for $\text{HoMn}_{1-x}\text{Ga}_x\text{O}_3$ over the temperature range $1.8 \text{ K} < T < 7 \text{ K}$. For all samples, the derivatives show a peak near $T_2 \approx 5 \text{ K}$, which is due to Ho^{3+} magnetic order.

Figure 6(a) shows the temperature dependence of the ther-

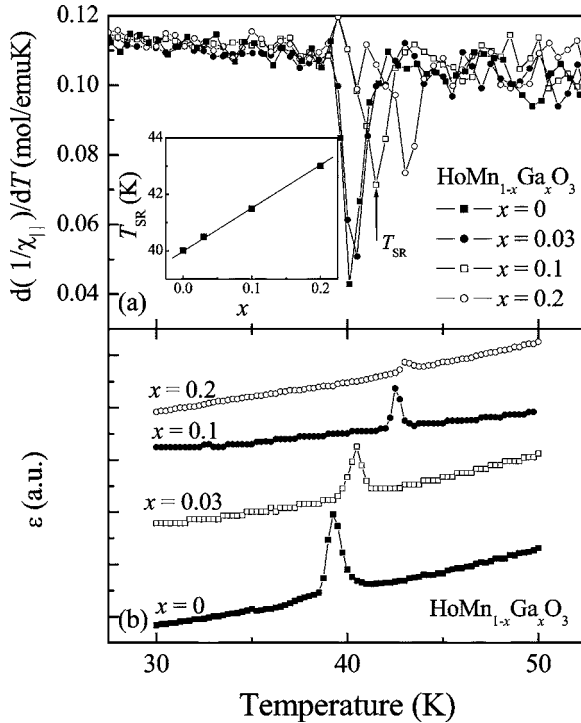


FIG. 4. Temperature dependences of (a) $d(1/\chi_{||})/dT$ with $25 \text{ K} < T < 60 \text{ K}$ and (b) dielectric constant ϵ for $\text{HoMn}_{1-x}\text{Ga}_x\text{O}_3$. Inset of (a): Variation with x of T_{SR} for $\text{HoMn}_{1-x}\text{Ga}_x\text{O}_3$. Here, $\chi_{||}$ and ϵ were measured along the c axis.

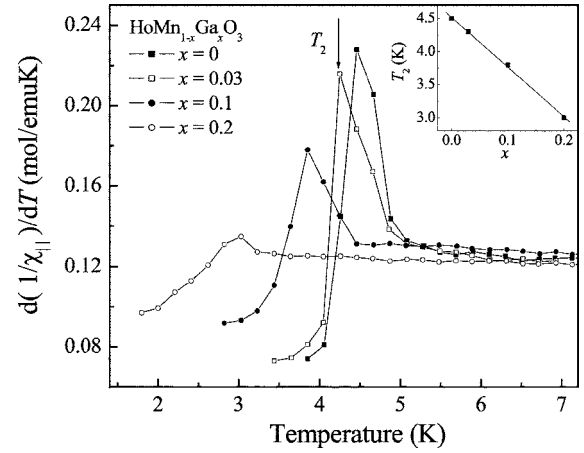


FIG. 5. Temperature dependences of $d(1/\chi_{||})/dT$ with $1.8 \text{ K} < T < 7 \text{ K}$ for $\text{HoMn}_{1-x}\text{Ga}_x\text{O}_3$. Inset: Variation with x of T_2 for $\text{HoMn}_{1-x}\text{Ga}_x\text{O}_3$.

mal conductivity of $\text{YMn}_{1-x}\text{Ga}_x\text{O}_3$. Several features are noteworthy: (i) at temperatures $T > T_N$, $\kappa(T)$ shows a relatively weak temperature dependence; moreover, for $\kappa(T)$ measured along the c axis, its magnitude increases with increasing x ; (ii) $\kappa(T)$ undergoes an increase at the onset of antiferromagnetic order below T_N ; T_N has been obtained independently from the susceptibility [Fig. 6(b)]. With increasing x , T_N decreases linearly; (iii) below T_N , the intensity of the $\kappa(T)$ peak is suppressed and the temperature of its maximum increases with increasing x . Figure 7 shows a similar behavior for the thermal conductivity of $\text{HoMn}_{1-x}\text{Ga}_x\text{O}_3$; its T_N also decreases linearly with increasing x .

IV. DISCUSSION

A. X-ray and thermal expansion

From high-temperature susceptibility or dielectric permittivity and loss measurements,^{2,6,18} the ferroelectric Curie temperature T_C for HoMnO_3 has been reported as 875 K , and for

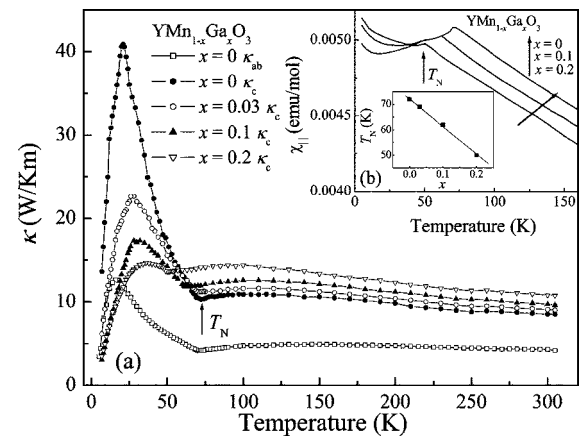


FIG. 6. (a) Temperature dependences of thermal conductivity and (b) molar magnetic susceptibility $\chi_{||}$ for $\text{YMn}_{1-x}\text{Ga}_x\text{O}_3$. Inset of (b): Variation with x of T_N for $\text{YMn}_{1-x}\text{Ga}_x\text{O}_3$. Here κ_{ab} and κ_c were measured along a - b plane and c axis, respectively.

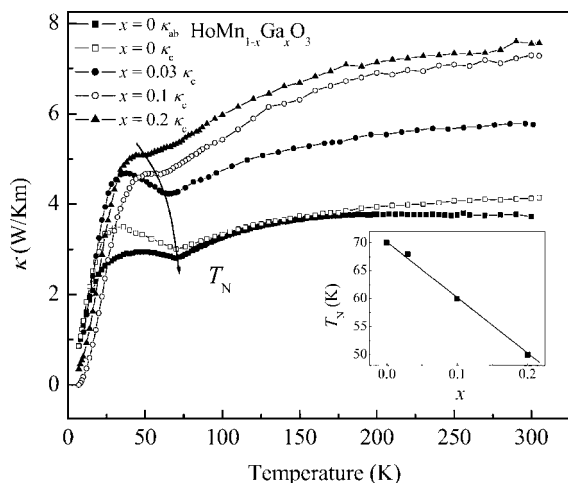


FIG. 7. Temperature dependences of thermal conductivity for $\text{HoMn}_{1-x}\text{Ga}_x\text{O}_3$. Inset: Variation with x of T_N for $\text{HoMn}_{1-x}\text{Ga}_x\text{O}_3$.

YMnO_3 as 915 K or 935 K. From high-temperature XRD studies, Lukaszewicz and Karut-Kalicinska¹⁹ reported small anomalies of lattice constants in the region 620 to 680 °C for YMnO_3 . Recently, Katsufuji *et al.*²⁰ reported a linear negative thermal expansion along the c direction of YMnO_3 , but actually the data show a slope change around 900 K; their data are replotted as “×” in Fig. 2(b). Our XRD and TMA measurements clearly show slope changes for the thermal expansion along the c direction at 875 K and 900 K for HoMnO_3 and YMnO_3 , respectively; these temperatures are consistent with the reported T_C values. Geller *et al.*²¹ have reported that RGaO_3 is isostructural with RMnO_3 , but with a larger c and smaller a . This observation is consistent with an increasing c/a ratio with increasing x in our $\text{RMn}_{1-x}\text{Ga}_x\text{O}_3$ samples. A larger c axis should accommodate a larger displacement of the R^{3+} ions below T_C than that in RMnO_3 (Ref. 22). Accordingly, the temperature of the slope change in Figs. 2 and 3 increases with x , which shows an increase in T_C as the c axis increases.

The thermal expansion coefficients $(\Delta c/\Delta T)/c$ shown in Fig. 8 for $x=0$ and 0.2 were obtained by fitting the lattice constant vs temperature data to a linear function. The absolute value of the coefficients above T_C are larger than those below T_C . A larger thermal expansion coefficient in the interval $T_C < T < T_1$ than below T_C implies that the c -parameter contraction introduced by the cooperative MnO_5 rotations is reduced by the R^{3+} -ion displacements along the c axis.

B. Susceptibility and dielectric constant

The dielectric constant ϵ along the c axis shows a sharp peak at T_{SR} in Fig. 4(b) and correlates with a peak in $d(1/\chi_{\parallel})/dT$ at T_{SR} in Fig. 4(a), which provides clear evidence of a coupling between the R^{3+} -ion ferroic displacements and the ordering of the Mn^{3+} -ion spins; a 90° rotation of the Mn^{3+} -ion spins occurs at this temperature.³ A $T_{\text{SR}}=40$ K in our HoMnO_3 crystal is the same as that recently reported from neutron measurements.⁴ Instead of decreasing to lower temperature with Ga doping as does T_N , T_{SR} moves to a higher temperature in $\text{HoMn}_{1-x}\text{Ga}_x\text{O}_3$. The

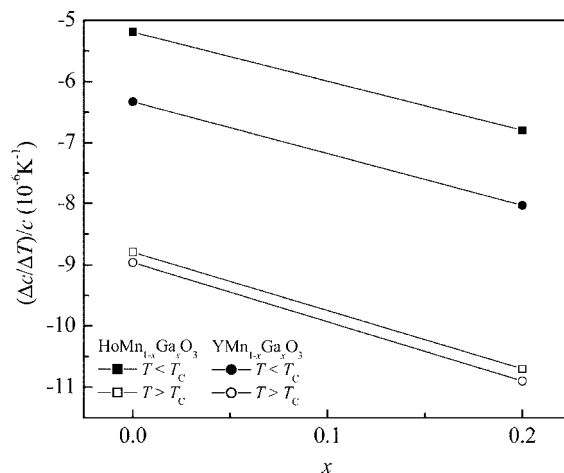


FIG. 8. Thermal expansion coefficients along c axis for $\text{RMn}_{1-x}\text{Ga}_x\text{O}_3$ ($x=0$ and 0.2).

increase of T_C with Ga doping has confirmed the enhancement with x of the R^{3+} -ion ferroic displacements, which increase with decreasing temperature at any given T below T_C . Therefore, the increase of T_{SR} with x clearly supports the conjecture that T_{SR} occurs at a critical R^{3+} -ion displacement. The expansion of the c axis with decreasing temperature can relieve the interplane spin-spin dipole interactions in HoMnO_3 (Ref. 10) to act as the driving force behind the spin-reorientation of the Mn^{3+} array. On the other hand, the decrease with x in the magnitude of the peak in $\epsilon(T)$ at T_{SR} shows that the reduced magnetic order parameter at T_{SR} lowers the coupling of the spin reorientation to the ferroic Ho^{3+} -ion displacements.

Long-range magnetic ordering of the Ho^{3+} -ion spins is accompanied by a 90° rotation of the Mn spins at T_2 within 0.3 K of the Ho-spin ordering temperature.¹² The decreases with x of T_2 like T_N and the magnitude of the peak in $d(1/\chi_{\parallel})/dT$ at T_2 suggest that the ordering of the Ho^{3+} -ion spins is coupled to the Mn^{3+} -ion order and depends on the 90° spin rotation and in-phase c axis order to be realized.

C. Thermal conductivity

Ga doping dilutes the dominant Mn-Mn interactions in the a - b plane, so T_N decreases with increasing x for $\text{RMn}_{1-x}\text{Ga}_x\text{O}_3$.

Above T_N , the thermal conductivity $\kappa(T)$ is dominated by the phonon contribution described by the Debye model,²³

$$\kappa_{ph} = (k_B/2\pi^2v)(k_B)^3T^3 \times \int_0^{\theta_D/T} dx \tau(\omega, T)x^4 e^x / (e^x - 1)^2 \quad (1)$$

where $\tau(\omega, T)$ is the mean lifetime of a phonon, θ_D is the Debye temperature, and v is the average sound velocity. This formula approaches a $1/T$ law at high temperatures, usually for $T > \theta_D/4$, as is seen in $\kappa(T)$ for the diamagnetic insulator LaGaO_3 .²⁴ The nearly temperature-independent and suppressed $\kappa(T)$ for YMnO_3 obviously deviates from the $1/T$ law. Sharma *et al.*¹⁷ have suggested that regions of short-

range magnetic order above T_N can lead to a nanoscale inhomogeneous strain that scatters acoustic phonons. The exchange striction associated with magnetic order introduces a strong spin-lattice interaction that is amplified where there is spin-interaction frustration.²⁴ The data for YMnO₃ and HoMnO₃ of Figs. 6 and 7 support this model. Of particular interest is the observation in these figures of an increase in $\kappa(T)$ above T_N with Ga doping. Normally, the effect of doping is to introduce an impurity scattering that lowers $\kappa_{ph}(T)$ as is illustrated, for example, by the perovskite LaMn_{1-x}Ga_xO₃ (Ref. 25). In YMnO₃ and HoMnO₃, dilution of the Mn-Mn interaction by Ga doping reduces the temperature range of short-range magnetic order above T_N , thereby reducing the spin-lattice interaction in the paramagnetic phase. This effect is stronger than the effect of impurity scattering, so $\kappa(T)$ increases with Ga doping above T_N .

The strong low-temperature peak of $\kappa_c(T)$ below T_N of YMnO₃ shows that long-range magnetic order restores $\kappa_{ph}(T)$ and may introduce a contribution by magnons. The magnitude of the peak in $\kappa_c(T)$ of YMnO₃ reflects the quality of our crystal, and a greater suppression of $\kappa_{ab}(T)$ is consistent with stronger spin-lattice interactions in the Mn basal planes.

V. CONCLUSIONS

Ga doping in the hexagonal RMn_{1-x}Ga_xO₃ compounds increases the ferrielectric transition temperature T_C and the

Mn-spin reorientation temperature T_{SR} while lowering T_N of the Mn array and the temperature T_2 of long-range order of the Ho³⁺-ion moments, which is associated with a second 90° reorientation of the Mn³⁺-ion spins. These observations reveal the existence of an important coupling of the Ho³⁺-ion spins and the Mn³⁺-ion magnetic order and support the conjecture that the spin reorientation at T_{SR} is driven by a critical R^{3+} -ion displacement that is controlled by the magnitude of the cooperative bipyramidal rotation found below T_1 . A larger c axis thermal contraction in the interval $T_C < T_1$ than below T_C suggests that the energy required to induce the ferroic R^{3+} -ion displacements reduces, below T_C , the magnitude of the cooperative bipyramidal rotations. A reduced suppression with x of the thermal conductivity $\kappa(T)$ above T_N confirms the importance of short-range spin-lattice interactions in a geometrically frustrated spin system.

ACKNOWLEDGMENTS

The authors are grateful to Dr. J. S. Swinnea for help with the high temperature XRD measurements, Dr. J.-S. Zhou for helpful discussions, and to the National Science Foundation and the Robert A. Welch Foundation of Houston, Texas, for financial support.

-
- ¹B. B. Van Aken, T. T. M. Palstra, A. Filippetti, and N. A. Spaldin, *Nat. Mater.* **3**, 164 (2004).
²P. Coeuré, P. Guinet, J. C. Peuzin, G. Buisson, and E. F. Bertaut, *Proceedings of the International Meeting on Ferroelectricity*, edited by V. Dvorák, A. Fousková, and P. Glogar (Institute of Physics of the Czechoslovak Academy of Science, Prague, 1966) Vol. 1, pp. 332–340.
³M. Fiebig, Th. Lottermoser, and R. V. Pisarev, *J. Appl. Phys.* **93**, 8194 (2003).
⁴O. P. Vajk, M. Kenzelmann, J. W. Lynn, S. B. Kim, and S.-W. Cheong, *Phys. Rev. Lett.* **94**, 087601 (2005).
⁵B. Lorenz, F. Yen, M. M. Gospodinov, and C. W. Chu, *Phys. Rev. B* **71**, 014438 (2005).
⁶I. G. Ismailzade and S. A. Kizhaev, *Sov. Phys. Solid State* **7**, 236 (1965).
⁷M. Fiebig, D. Fröhlich, K. Kohn, St. Leute, Th. Lottermoser, V. V. Pavlov, and R. V. Pisarev, *Phys. Rev. Lett.* **84**, 5620 (2000).
⁸M. Fiebig, C. Degenhardt, and R. V. Pisarev, *J. Appl. Phys.* **91**, 8867 (2002).
⁹Th. Lottermoser, M. Fiebig, D. Fröhlich, St. Leute, and K. Kohn, *J. Magn. Mater.* **226–230**, 1131 (2001).
¹⁰Th. Lottermoser, Th. Lonkai, U. Amann, D. Hohlwein, J. Ihringer, and M. Fiebig, *Nature* **430**, 541 (2004).
¹¹A. Muñoz, J. A. Alonso, M. J. Martínez-Lope, M. T. Casáis, J. L. Martínez, and M. T. Fernández-Díaz, *Chem. Mater.* **13**, 1497 (2001).
¹²F. Yen, C. R. dela Cruz, B. Lorenz, Y. Y. Sun, Y. Q. Wang, M. M. Gospodinov, and C. W. Chu, *Phys. Rev. B* **71**, 180407(R) (2005).
¹³Seongsu Lee, A. Pirogov, Jung Hoon Han, J.-G. Park, A. Hoshikawa, and T. Kamiyama, *Phys. Rev. B* **71**, 180413(R) (2005).
¹⁴C. R. dela Cruz, F. Yen, B. Lorenz, Y. Q. Wang, Y. Y. Sun, M. M. Gospodinov, and C. W. Chu, *Phys. Rev. B* **71**, 060407(R) (2005).
¹⁵B. Lorenz, A. P. Litvinchuk, M. M. Gospodinov, and C. W. Chu, *Phys. Rev. Lett.* **92**, 087204 (2004).
¹⁶T. Katsufuji, S. Mori, M. Masaki, Y. Moritomo, N. Yamamoto, and H. Takagi, *Phys. Rev. B* **64**, 104419 (2001).
¹⁷P. A. Sharma, J. S. Ahn, N. Hur, S. Park, Sung Baek Kim, Seongsu Lee, J.-G. Park, S. Guha, and S.-W. Cheong, *Phys. Rev. Lett.* **93**, 177202 (2004).
¹⁸V. A. Bokov, G. A. Smolenskii, S. A. Kizhaev, and I. E. Mylnikova, *Sov. Phys. Solid State* **5**, 2646 (1964).
¹⁹Kazimierz Lukaszewicz and Jaroslawa Karut-Kalicinska, *Ferroelectrics* **7**, 81 (1974).
²⁰T. Katsufuji, M. Masaki, A. Machida, M. Moritomo, K. Kato, E. Nishibori, M. Takata, M. Sakata, K. Ohoyama, K. Kitazawa, and H. Takagi, *Phys. Rev. B* **66**, 134434 (2002).
²¹B. S. Geller, J. B. Jeffries, and P. J. Curlander, *Acta Crystallogr.* **B31**, 2770 (1975).
²²S. C. Abrahams, *Acta Crystallogr.* **B57**, 485 (2001).
²³R. Berman, *Thermal Conduction in Solids* (Clarendon Press, Oxford, 1976).
²⁴J.-S. Zhou and J. B. Goodenough, *Phys. Rev. B* **66**, 052401 (2002).
²⁵J.-S. Zhou, H. Q. Yin, and J. B. Goodenough, *Phys. Rev. B* **63**, 184423 (2001).